Synaptotagmin-7 enhances calcium-sensing of chromaffin cell granules and slows discharge of granule cargos

Mounir Bendahmane[1+], Alina Chapman-Morales[1+], Alex J.B. Kreutzberger[2], Noah A. Schenk[1], Ramkumar Mohan[1], Shreeya Bakshi[1], Julie Philippe[1], Shuang Zhang[1], Volker Kiessling[2], Lukas K. Tamm[2], David R. Giovannucci[3], Paul M. Jenkins[1], Arun Anantharam[1*]

[1]Department of Pharmacology, University of Michigan, Ann Arbor, MI 48109

[2]Center for Membrane and Cell Physiology and Department of Molecular Physiology and Biological Physics, University of Virginia, Charlottesville, VA 22908

[3]Department of Neuroscience, University of Toledo Medical School, Toledo, OH 43606

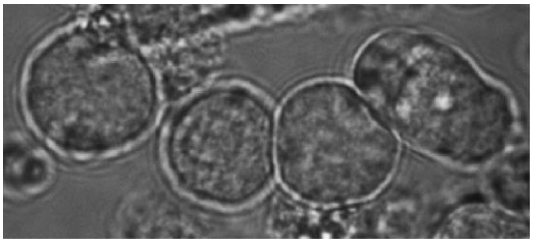

Supplementary Figure 1. **Mouse chromaffin cells 24 hours after plating on Matrigel coated glass bottom dishes.** Healthy, transfected chromaffin cells are selected for TIRFM experiments based on their oblong shape and tendency to cluster.

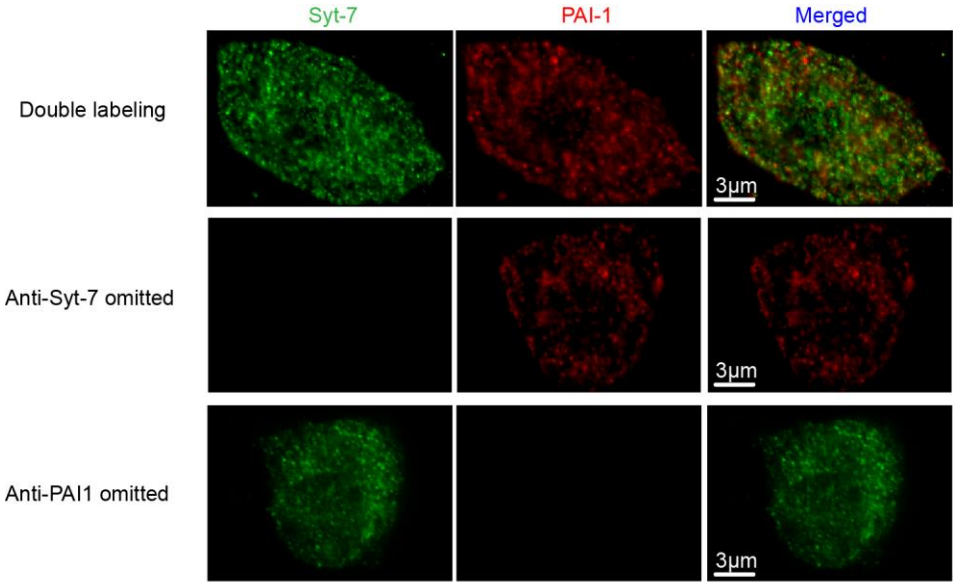

Supplementary Figure 2. **Validation of immunocytochemical-staining method using two primary antibodies raised in rabbit.** Images show double-labeling for Syt-7 and PAI-1 (top row, image from figure 1). No labeling was seen for Syt-7 when the antibody was omitted. No labeling for PAI-1 was seen when the antibody was omitted (Syt-7, middle row and PAI-1 bottom row; 1 primary cell preparation).

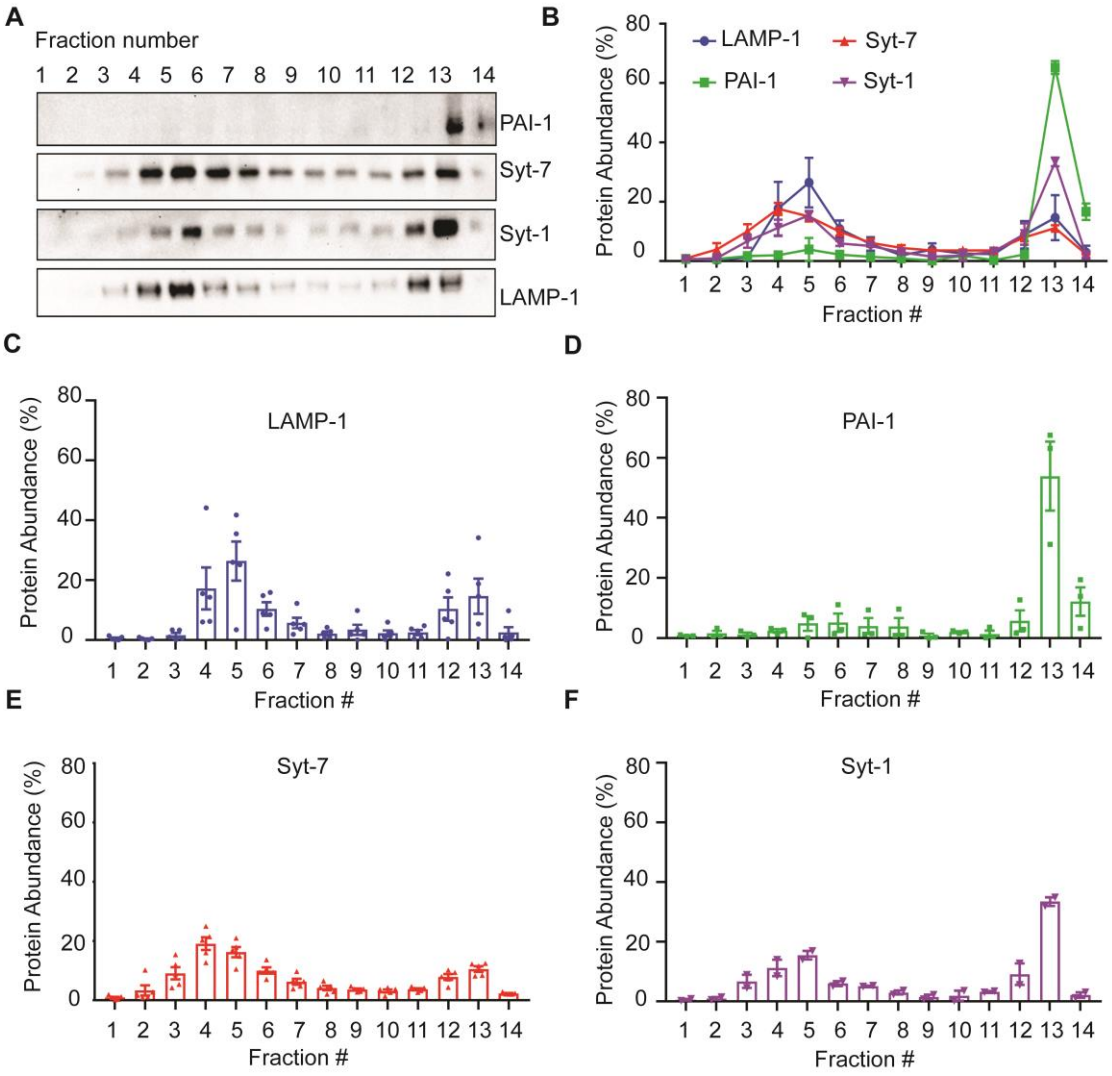

Supplementary Figure 3. A. Representative blot showing bands corresponding to protein of interest (PAI-1: 45 kDa, Syt-7: 45 kDa, Syt-1: 65 kDa, and LAMP-1: 120 kDa). **B.** Expression level of PAI-1 (n = 3), Syt-7 (n = 5), Syt-1 (n = 2), and LAMP-1 (n = 5) shown as percentage of protein abundance in each subcellular fraction of bovine chromaffin cells (n represents individual fractionation experiments; 3 primary bovine cell preparations) **C-F**. Individual scatter box-plot graphs for LAMP-1, PAI-1, Syt-7 and Syt-1 respectively. Data are represented as mean ± SEM.

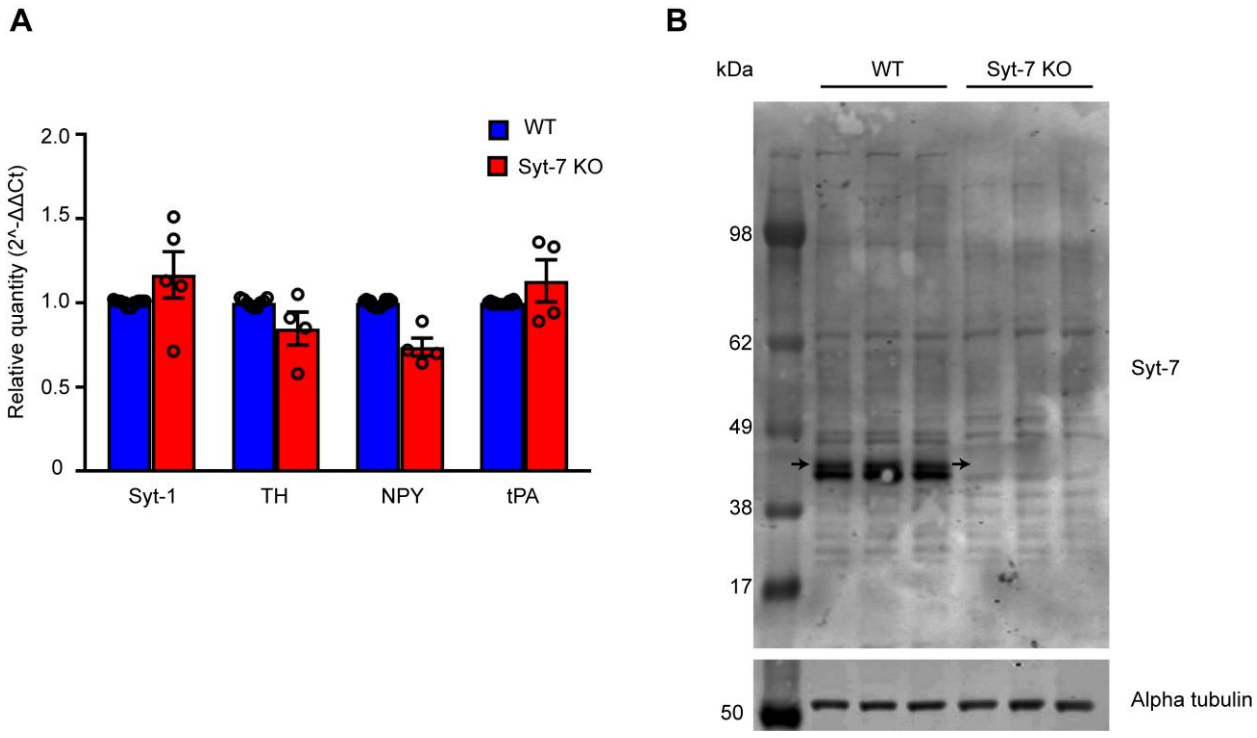

Supplementary Figure 4. A. Expression of Syt-1, TH, NPY and tPA transcripts in WT and Syt-7 KO chromaffin cells. For each individual experiment, 4 WT and 4 KO adrenal medullas were homogenized, mRNA was extracted, and RT-qPCR was performed on the samples for Syt-1 (n = 5), NPY (n = 3), tPA (n = 3), TH (n = 3), and Syt-7 (n = 2; n represents individual experiments for all). Syt-7 transcript was not detected using the primers shown in Table 1. Expression of Syt-1 mRNA was not significantly different in WT and KO cells (Student's t-test, $p > 0.05$). **B.** Western blot analysis was performed on WT and Syt-7 KO adrenal glands. Black arrow indicates the region where the approximately 45 kDa Syt-7 α variant should be observed (Chakrabarti et al., 2003; Sugita et al., 2001). This band is present in the WT lanes but not in the Syt-7 KO lanes.

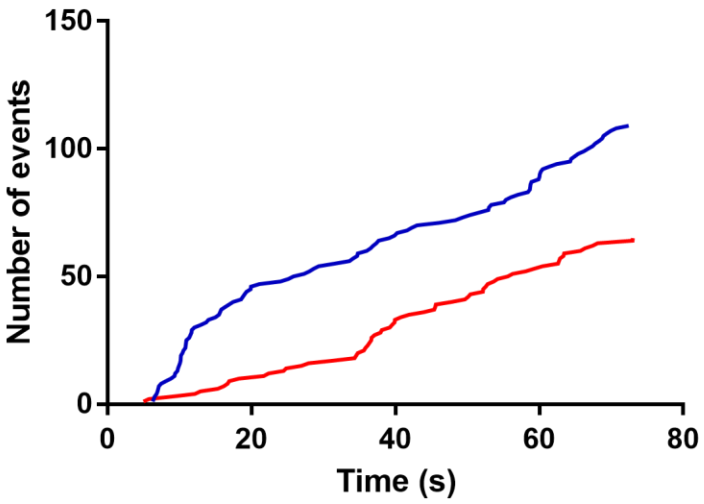

Supplementary Figure 5. NPY-pHl was overexpressed in WT and Syt-7 KO chromaffin cells. Secretion was triggered by local perfusion of 100 mM KCl. Cumulative frequency distribution showing the time at which fusion events occurred in WT (blue) and Syt-7 KO (red) (n=8 cells for WT and n=5 cells for KO; 4 primary cell preparations for both groups). Both WT and KO cells secrete throughout the stimulation period, although the total number of fusion events is greater in WT cells.

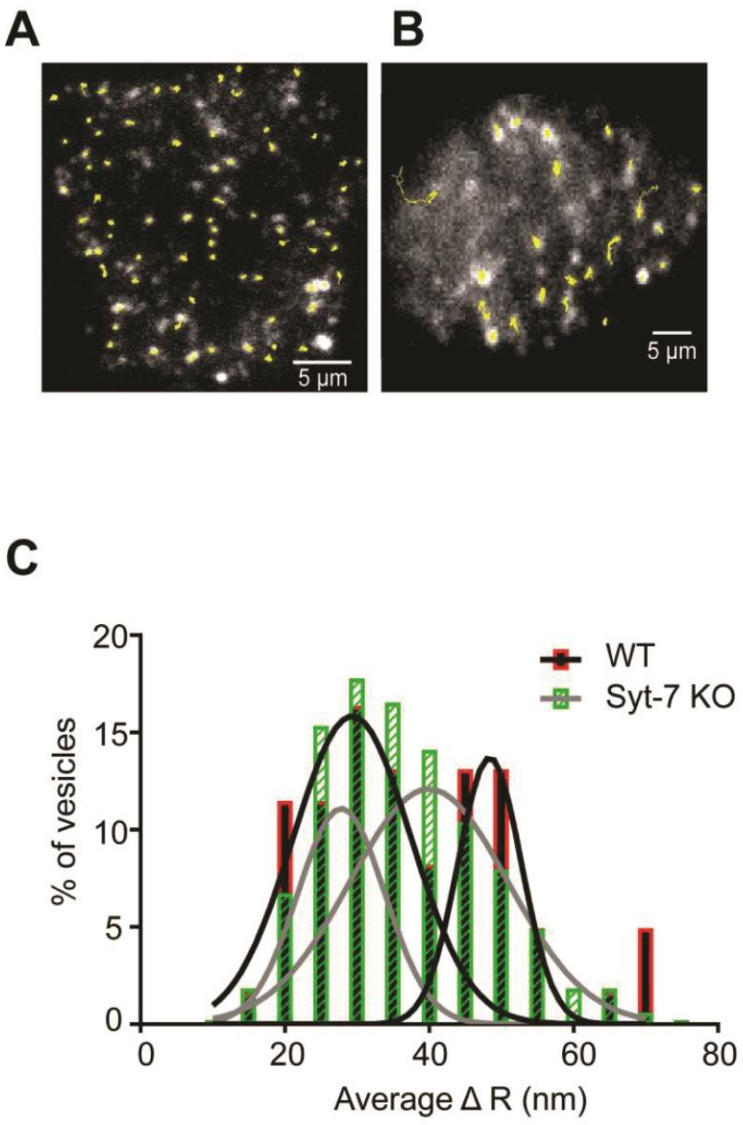

Supplementary Figure 6. An analysis of granule motion in WT and Syt-7 KO cells.

A-B. Representative tracks of WT (A) and Syt-7 KO (B) granules. **C.** Average mean frame-to-frame displacement of slower and faster WT granule populations, 29.32 +/- 1.41 nm/frame and 48.39 +/- 1.13 nm respectively, and slower and faster Syt-7 KO granules, 27.82 +/- 0.59 nm/frame, and 39.97 +/- 3.76 nm/frame, respectively.

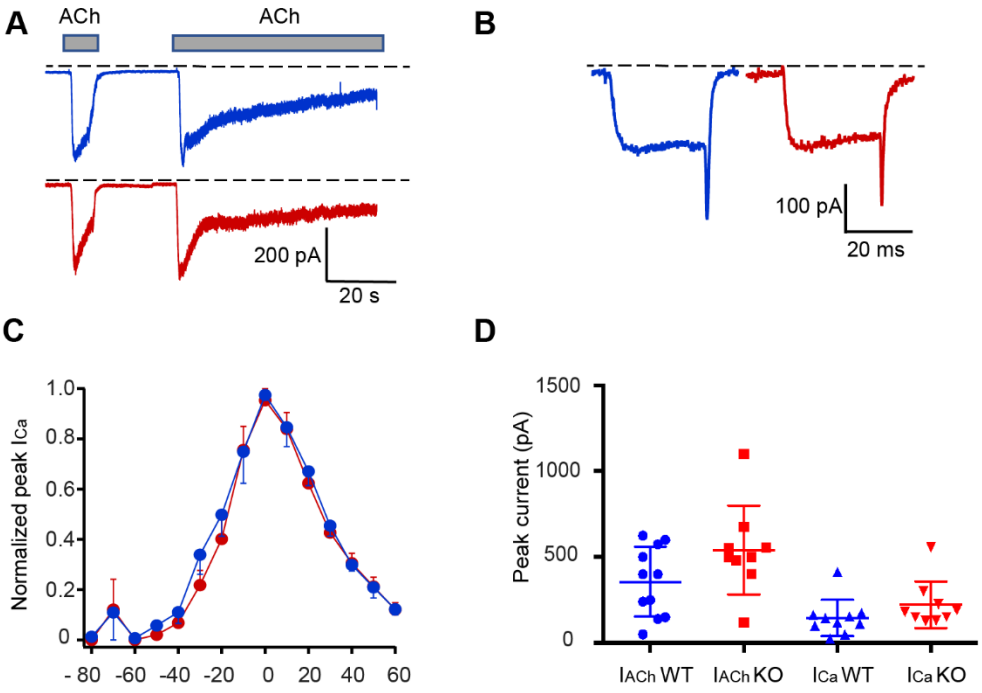

Supplementary Figure 7. Cholinergic currents and depolarization-evoked Ca^{2+} currents are similar in WT and KO cells. Whole-cell patch clamp recordings were performed in WT (blue) and Syt-7 KO (red) cells. **A-B.** Representative cholinergic currents (I_{ACh}) (**A**) and Ca^{2+} currents (I_{Ca}) (**B**). Currents were evoked by application of 100 µM ACh (**A)** or by a 30 ms step-depolarization (**B**) from a holding potential of -90 mV. **C.** Voltage-dependent activation and inactivation of the I_{Ca} in WT and Syt-7 KO cells. Each point represents the mean peak amplitude of the I_{Ca} (n = 7 evoked currents) evoked by a 30 ms step depolarization to test potentials of different amplitudes from a holding potential of -90 mV and normalized to the maximal response of each cell. **D.** A comparison of the mean data and range of peak amplitudes of I_{ACh} and I_{Ca} evoked in WT and Syt-7 KO cells. Mean Syt-7 KO current amplitudes were not altered compared to WT cells (Student's t-test, $p > 0.05$).

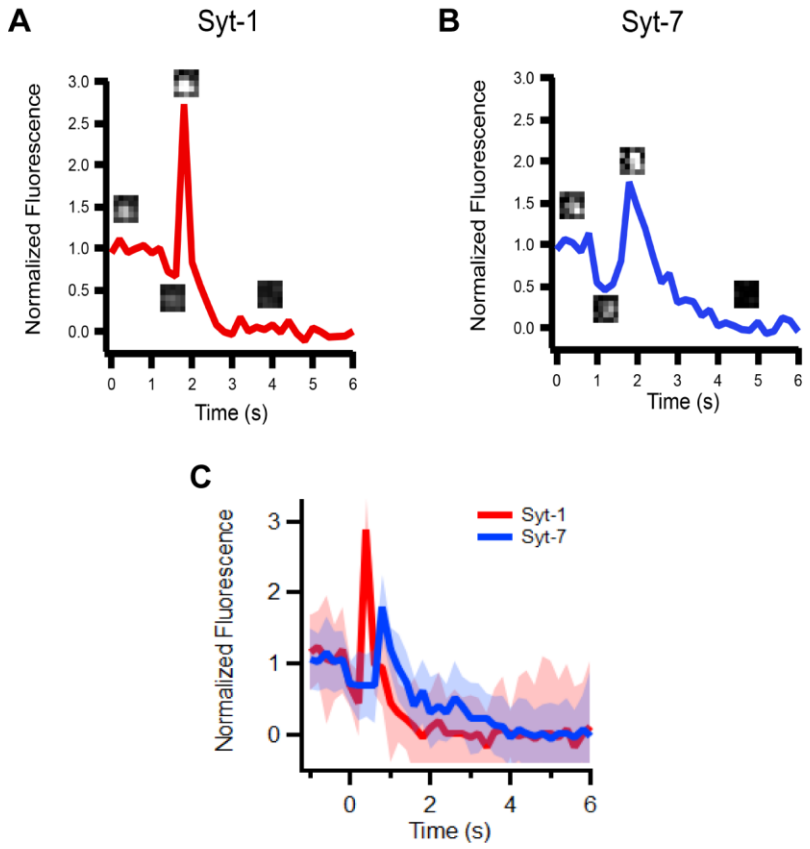

Supplementary Figure 8. **A-B**. Images from individual NPYmRuby release events. **C**. An overlay of the averaged NPYmRuby "line shapes" is shown (Kreutzberger *et al.* 2017b; Kreutzberger *et al.* 2019).

Supplementary Movie 1. Example of a WT mouse chromaffin cell expressing NPY-GFP and stimulated with 100 mM KCl. Secretion was imaged with a TIRF microscope (see Methods).

Supplementary Movie 2. Example of a WT mouse chromaffin cell expressing NPY-GFP and stimulated with 100 mM ACh. Secretion was imaged with a TIRF microscope (see Methods).

Supplemental Table 1. List of Chemicals/Materials

Chemical/materials	Vendor	Catalog number	notes
Fluriso (Isofluorane)	Vetone	H03A18B	
Sodium Chloride	Fisher BioReagents	BP-358-212	
Potassium Chloride	EMD Chemicals	PX1405-1	
Glucose	Sigma	G8270	
Potassium Phosphate monobasic	EMD Chemicals	PX1565-1	
Potassium Phosphate Dibasic	Sigma	P966	
HEPES	Sigma	H3375	
D-Mannitol	Sigma	M4125	
Micro scissors	World Precision Instruments	14124-G	
Papain	Worthington Biochemical	LS003126	
Bovine Serum Albumin (BSA)	Sigma-Aldrich	A7906	
Dulbecco's Modified Eagle's Medium	ThermoFisher Scientific		F12 [+] L-glutamine [+] 15mM HEPES
Fetal Bovine Serum (FBS)	Gibco by Life Technologies	10437-028	
Calcium Chloride	Sigma	C1016	
Magnesium Chloride	Fisher BioReagents	BP214	
Acetylcholine	Sigma	A6625	
Paraformaldehyde	Polysciences	18814	
Ammonium Chloride	Sigma	A9434	
Gelatin	Sigma	G9391	
MES	Sigma	M3671	

Rabbit polyclonal Anti-syt-7 antibody	Synaptic Systems	105 173 RRID: AB_887838	1:1200
Polyclonal anti-PAI-1	Abcam	66705 RRID:AB_1310540	1:1000
Uncongugated F(ab')2-Goat anti-Rabbit IgG	Invitrogen, Thermofisher	A24539 RRID:AB_2536007	1:300
Normal Rabbit Serum	Invitrogen, Thermofisher	016101 RRID:AB_2532937	
Mouse anti-alpha tubulin	Cedarlane	CLT 9002 RRID:AB_10060319	1:10000
Mouse monoclonal anti-LAMP-1	Abcam	Ab25630 RRID:AB_470708	1:500
Rabbit polyclonal anti-LAMP-1	Abcam	Ab24170 RRID:AB_775978	1:1000
Mouse Monoclonal Anti-Syt-1	Synaptic Systems	105 011 RRID:AB_887832	1:1200
Licor fluorescent secondaries	IRDye 800CW Donkey Anti-rabbit	C9012905	1:10000
Licor fluorescent secondaries	IRDye 680CW Donkey Anti Rabbit	C92568073	1:10000
anti-mouse HRP	GE healthcare	NXA931V RRID: AB_2721110	1:5000
anti-rabbit HRP	GE healthcare	NA934V RRID: AB_772206	1:5000
SDS	Sigma Life Sciences	L3771	
Glass Bottom Dishes	MatTek Corporation, Ashland MA	P35G-1.5-14-C	
Matrigel	Corning, NY	356230	
Sucrose	Sigma	84100	
Tris HCl	Roche Diagnostics	10-708-976-001	
EDTA	Fisher Chemical	S311-100	
mycSyt-7 plasmid	Gifted by Dr. Thomas Sudhof		
NPY-pHluorin	Gifted from Dr. Ronald Holz	Vector: pEGFP-N1	Kanamycin resistance
NPY-GFP	Gifted from Dr. Ronald Holz	Vector: pEGFP-N1	Ampicillin resistance
NPY-mRuby	Gifted from Ronald Holz	Vector: pEGFP-N1	Ampicillin resistance
tPA-pHl	Gifted from Ronald Holz	Vector: pEGFP-N1	Ampicillin resistance
Sylgard elastomer	EMS, Hatfield, PA	24236-10	